PERGAMON

Journal of Structural Geology 24 (2002) 289–295

JOURNAL OF STRUCTURAL GEOLOGY

www.elsevier.com/locate/jstrugeo

Backlimb trishear: a kinematic model for curved folds developed over angular fault bends

Ernesto O. Cristallini[a,b,*], Richard W. Allmendinger[a]

[a]*Department of Earth and Atmospheric Sciences, Cornell University, Ithaca, NY 14853, USA*
[b]*CONICET — Departamento de Ciencias Geológicas, Universidad de Buenos Aires, Argentina*

Received 28 June 2000; revised 1 January 2001; accepted 6 April 2001

Abstract

Numerous analog models and some natural examples display smoothly curving backlimb fold hinges over sharp, angular bends in the underlying thrust surface. We present a new kinematic model that can reproduce this geometry by defining a triangular zone focused on the fault bend. The model presupposes incompressible flow in the triangular zone and makes common assumptions about velocities on either side of the fault bend. Either symmetric or asymmetric triangular zones can be defined, with parallel kink folding and similar folding being special cases of the two, respectively, where the apical angle of the triangular zone is zero. The results of the numerical model compare well to analog experiments. The model is conceptually analogous to forelimb trishear at the tip of a propagating fault and hence we refer to it as 'backlimb trishear'. © 2001 Published by Elsevier Science Ltd.

Keywords: Backlimb trishear; Kinematic model; Angular fault bends; Growth strata

1. Introduction

The assumption that cross-sectional area must be conserved during deformation is the basis for the majority of 2D fault-fold models. For example, parallel kink fold kinematics has been used extensively for analyzing compressive structures during the past 20 years because it is simple, easy to apply, and represents very well many structures found in nature. However, kink models (Suppe, 1983; Suppe and Mendwedeff, 1990) fail to explain curved fold hinges and bedding thickness changes commonly observed both on the forelimb and over footwall ramps on the backlimb. Inclined shear, similar fold kinematics (White et al., 1986) can produce thickness changes and generate curved limbs by using a curved fault. Trishear kinematics, proposed by Erslev (1991), can simulate curved forelimbs from a straight or curved fault.

Until now, however, no existing kinematic model is able to produce curved backlimbs without using a curved fault. Yet natural structures and analog models (Morse, 1977; Serra, 1977; Chester et al., 1991) commonly display this geometry (Fig. 1a and b). Furthermore, mechanical models of fault-bend folds (Fig. 1c) also produce smoothly curved beds over angular fault bends (Berger and Johnson, 1983; Johnson and Berger, 1989). In the interest of reconciling the idealized kink model with field, experiment, and mechanical theory, we present a new kinematic model for the backlimb. Our approach is conceptually similar to trishear (Erslev, 1991; Zehnder and Allmendinger, 2000) and permits us to model rounded folds that form above angular fault bends. Fault-bend kink models (Suppe, 1983) and inclined shear models (White et al., 1986) can be considered as special cases of the backlimb trishear kinematic proposed here.

The idea of the backlimb trishear is simply that the beds progressively rotate during deformation above an angular bend in the fault plane (Fig. 2a). The area where the beds rotate is constrained inside a triangular zone with its apex at the fault bend. With this behavior, beds near the fault will have sharper curvature than those far from the fault, similar to that observed in nature and experiment. Different velocity fields that conform to the assumption of area conserved can be found, and it is not necessary that the triangular zone be symmetric with respect to the fault-bend bisector. When the triangular zone is asymmetric, our model provides a convenient way of simulating back-thrusts such as those described by Serra (1977).

* Corresponding author. Corresponding address: Departamento de Ciencias Geológicas Ciudad Universitaria, Pabellon II, (C1428EHA), Ciudad de Buenos Aires, Argentina.

E-mail address: ernesto@gl.fcen.uba.ar (E.O. Cristallini).

0191-8141/01/$ - see front matter © 2001 Published by Elsevier Science Ltd.
PII: S0191-8141(01)00063-3

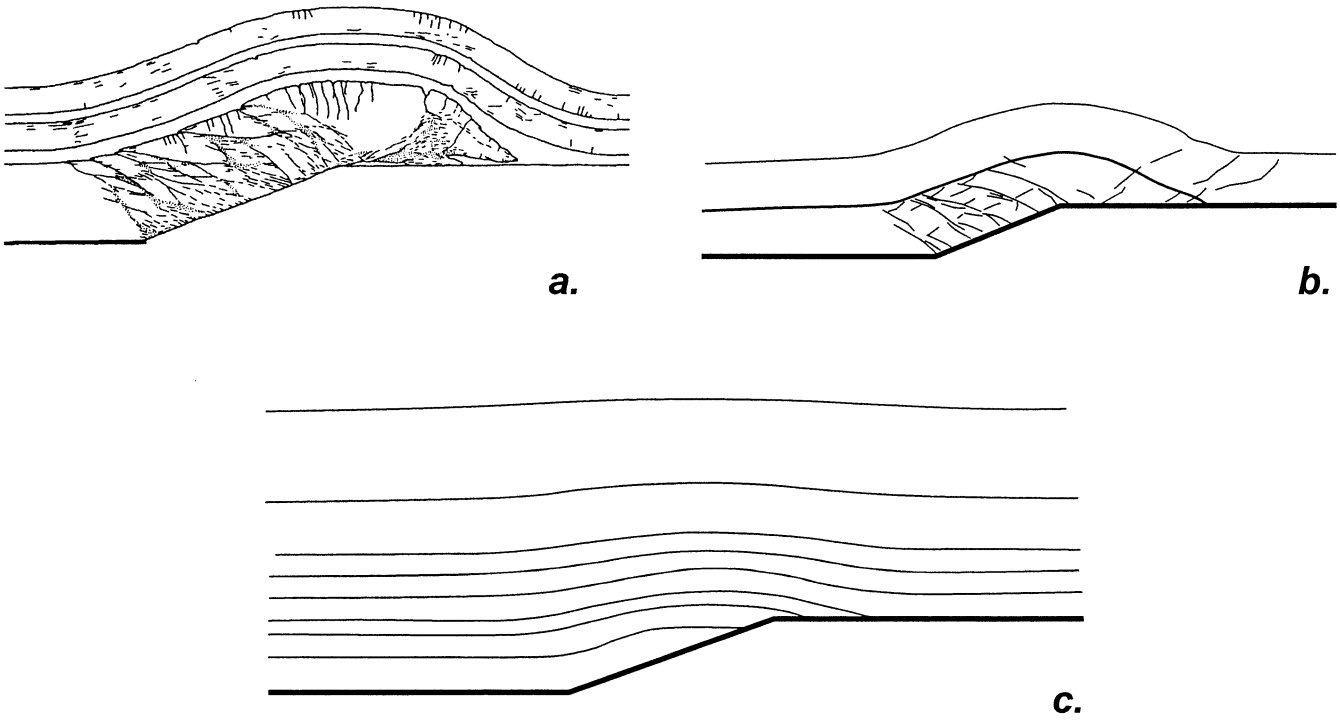

Fig. 1. Tracings of analog experiments and mechanical models of deformation over a flat-ramp transition. (a) Analog experiment carried out by Chester et al. (1991). (b) Analog experiment by Morse (1977). (c) Mechanical model of Berger and Johnson (1983) and Johnson and Berger (1989) calculated assuming viscous deformation of passive markers over a rigid footwall.

2. Implementation of a backlimb trishear

2.1. Coordinate transformations

To derive the velocity fields for backlimb trishear we define two coordinate systems: The first is a global coordinate system in which x represents the east or right-hand direction of the model and y represents the down direction (Fig. 2a and b). The backlimb triangular zone defines a local coordinate system where x' is the bisector of the apical angle of the triangular zone, y' is 90° counter-clockwise from x' (Fig. 2b) and the origin corresponds to the fault bend apex. The movement of the backlimb points of the model is calculated in the $x'y'$ coordinate system and then transformed to the xy coordinate system for visualization.

2.2. Velocity fields in the backlimb trishear

The boundary conditions for the backlimb triangular zone are (Fig. 2b):

$$V'_{0x} = V_0 \sin|\lambda_0| \mathrm{sgn}\lambda_0, \qquad V'_{0y} = -V_0 \cos|\lambda_0|, \qquad \text{for } y' = x' \tan\varphi,$$
$$V'_{1x} = V_1 \sin|\lambda_1| \mathrm{sgn}\lambda_1, \qquad V'_{1y} = -V_1 \cos|\lambda_1|, \qquad \text{for } y' = -x' \tan\varphi. \tag{1}$$

where 2φ is the backlimb triangular zone apical angle, and V_0 and V_1 are the velocities before and after the fault bend, respectively, given by:

$$V_1 = \frac{V_0 - \Delta V_0 \mathrm{sgn}\left(\frac{\theta}{2} - \alpha\right)}{\cos\theta} \qquad \text{where}$$
$$\Delta V_0 = \frac{V_0 \tan\theta \tan(|\frac{\theta}{2} - \alpha|)}{1 + \left[\tan\theta \tan\left(\left|\frac{\theta}{2} - \alpha\right|\right)\right]}. \tag{2}$$

θ is the angle between the two segments of fault, α is the asymmetry with respect to the bisector of both segments (α is negative backward) and λ_0 and λ_1 represent the angle between the fault plane and the y' axis before and after the fault bend, respectively (Fig. 2b and c):

$$\lambda_0 = \alpha - \frac{\theta}{2}, \qquad \lambda_1 = \alpha + \frac{\theta}{2}. \tag{3}$$

The velocities V_0 and V_1 are the same ($V_0 = V_1$) when the backlimb triangular zone is symmetric ($\alpha = 0$).

To find the velocity field inside the backlimb triangular zone that preserves area, we use the condition of flow incompressibility, specified by setting the divergence of the velocity field to zero (Mase and Mase, 1992; Hardy, 1995; Zehnder and Allmendinger, 2000):

$$\mathrm{div}\underline{V'} \equiv \frac{\partial V'_x}{\partial x} + \frac{\partial V'_y}{\partial y} = 0 \tag{4}$$

A simple, linear but non-unique V'_x field that satisfies the

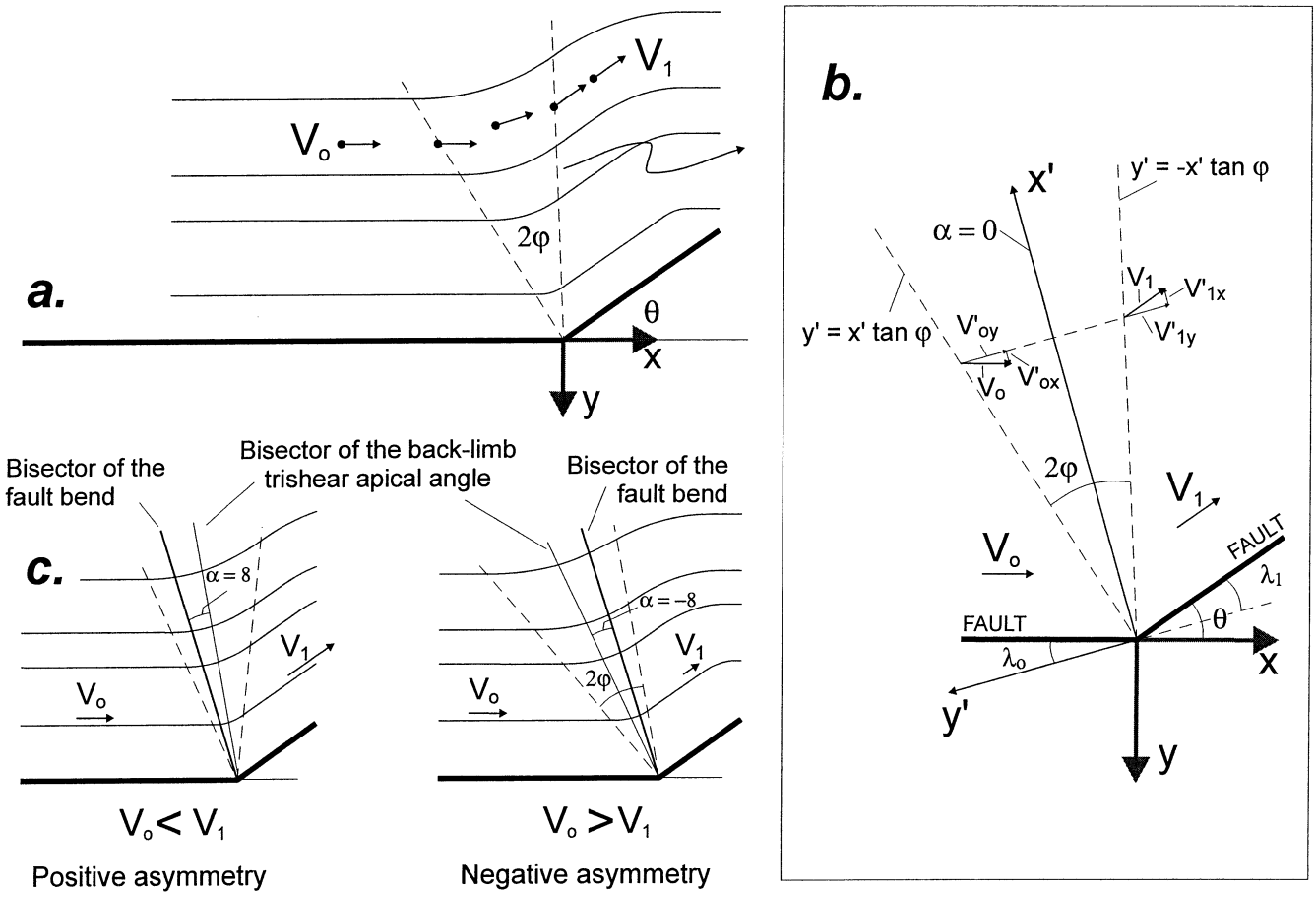

Fig. 2. (a) Backlimb trishear implies progressive rotation of the beds over an angular fault bend. The angle 2φ represents the apical angle and V_0 and V_1 the velocities on either side of the triangular zone. The axes xy represent the global coordinate system. (b) The angular relations and velocity components in the triangular zone ('local') coordinate system, $x'y'$. See text for discussion. (c) Definition of the asymmetry angle (α); in (a) and (b) the triangular zone is symmetric ($\alpha = 0$).

boundary conditions is:

$$V'_x = \frac{V'_{0x}}{2}\left[\frac{y'}{x'\tan\varphi} + 1\right] + \frac{V'_{1x}}{2}\left[\frac{y'}{x'\tan\varphi} + 1\right]. \quad (5)$$

Using incompressibility (Eq. (4)) and differentiating V'_x with respect to x' and then integrating the result with respect to y' we find the V'_y field:

$$V'_y = (V'_{0x} - V'_{1x})\left[\frac{1}{4\tan\varphi}\left(\frac{y'}{x'}\right)^2\right] + C. \quad (6)$$

The constant of integration is found by using one of the boundary conditions:

$$C = (V'_{1x} - V'_{0x})\left[\frac{1}{4\tan\varphi}\left(\frac{y'}{x'}\right)^2\right] - V'_{0y}. \quad (7)$$

3. Forward modeling

The iterative numerical calculations necessary to apply the above equations must be computed. For the forelimb, we use the trishear equations of Zehnder and Allmendinger (2000), which require the definition of another coordinate system where x'' is parallel to the fault near the tip-line, y'' is 90° counter-clockwise of x'', and the origin is in the tip-line. We can change all the variables pertinent to backlimb trishear: fault angle, apical angle, and displacement and the most important variables relevant to forelimb trishear: fault angle, apical angle, concentration (s), displacement and P/S (propagation to slip).

3.1. Symmetric backlimb trishear

Because backlimb trishear involves shear oblique to the bedding plane, the models will be area balanced but not necessarily line-length balanced. Bed thickness changes occur even in the symmetric cases ($\alpha = 0$) when the apical angle is greater than zero. When the apical angle is zero, there will be no changes in thickness and the backlimb will be exactly as the fault bend-fold model predicts (Suppe, 1983; Johnson and Berger, 1989; Hardy, 1995). Fig. 3a shows a case of symmetric backlimb trishear with a 30° apical angle where the beds are slightly thickened in the

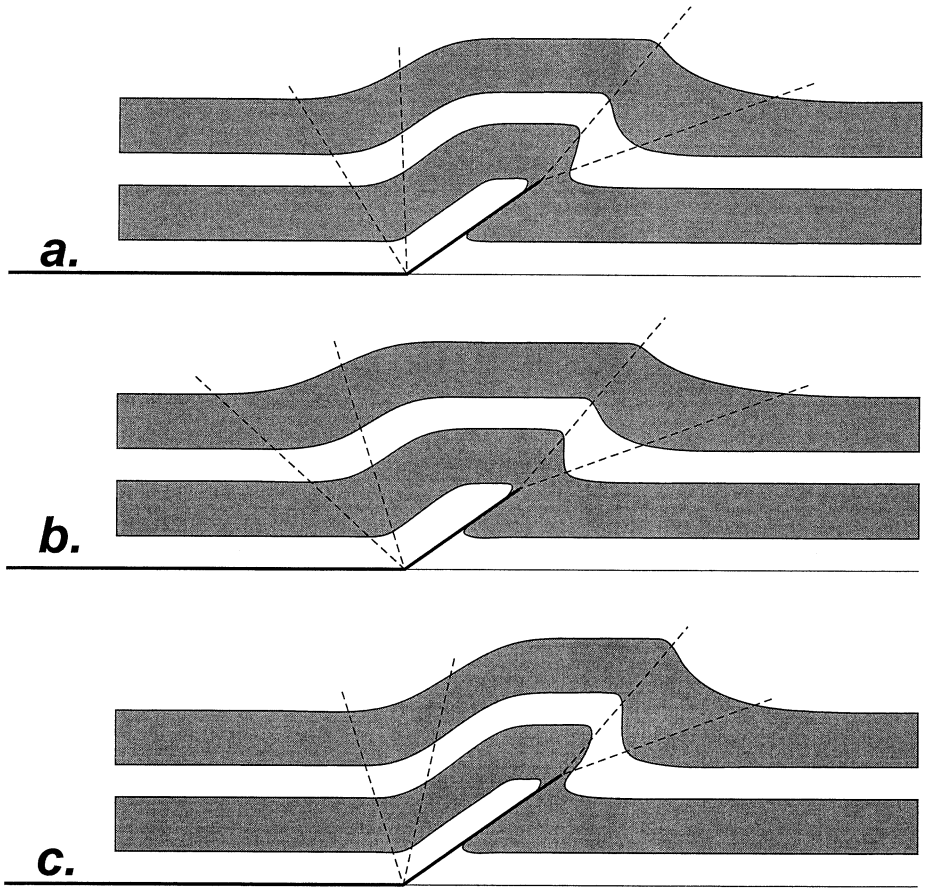

Fig. 3. Three examples of trishear fault-propagation folds where all the fore- and backlimb variables are the same except for the asymmetry of backlimb trishear. The fault angle is 35°, the forelimb trishear has an apical angle of 30° and a $P/S = 1.5$. The backlimb trishear apical angle is 30° and is symmetric in (a) ($\alpha = 0$) and asymmetric in (b) and (c) with $\alpha = -15$ and $\alpha = 15$, respectively.

hanging wall syncline and slightly thinned in the backlimb. With large apical angles, the thickness variations are more pronounced. The slip parallel to the fault plane is conserved on both sides of the backlimb trishear zone because the thickening and thinning balance out each other.

3.2. Asymmetric backlimb trishear

In the cases where the backlimb trishear is asymmetric with respect to the fault bend ($\alpha \neq 0$) the changes in thickness will be greater. Fig. 3b shows an asymmetric backlimb trishear ($\alpha = -15$; positive is toward the foreland) with 30° of apical angle, where the beds are clearly thickened in the hanging wall syncline and in the backlimb. Because part of the shortening is absorbed in this thickening, the slip parallel to the fault is not conserved across the backlimb trishear zone. The slip parallel to the fault will decrease to the right of the trishear zone, and only the slip parallel to the decollement is conserved as in the inclined shear (constant heave) model. The height of the crest will be less than in the symmetric example (compare Fig. 3a and b).

When the asymmetry is positive (Fig. 3c) the beds will be thinned in the hanging wall syncline and in the backlimb. Because of this, and to remain balanced, the slip parallel to the fault plane must increase to the right of the backlimb trishear zone to maintain constant heave. The crest will be higher than in the symmetric example (compare Fig. 3a and c). In the three examples of Fig. 3 the only variable that changes is the asymmetry of the backlimb trishear zone, however, the resulting folds are very different.

3.3. Growth-strata

In the backlimb trishear, the beds progressively rotate during deformation above the angular bend of the fault. Fig. 4a shows a trishear fault-propagation fold with $P/S = 1.5$ and a symmetric backlimb trishear with apical angle of 30° where the accumulation rate of the growth-strata is equal to the uplift rate. The growth-strata in the backlimb are progressively rotated and pinch-out on the crest of the anticline. The example of Fig. 4b shows the same structure but in this case the accumulation rate of the growth-strata is greater than the uplift rate. The progressive rotation of the growth-strata produces a smooth reduction of the thickness over the top of the anticline. For comparison, Fig. 4c and d represent the same basic geometry as Fig. 4a and b but using parallel-kink model for the backlimb and show that the pattern of growth-strata

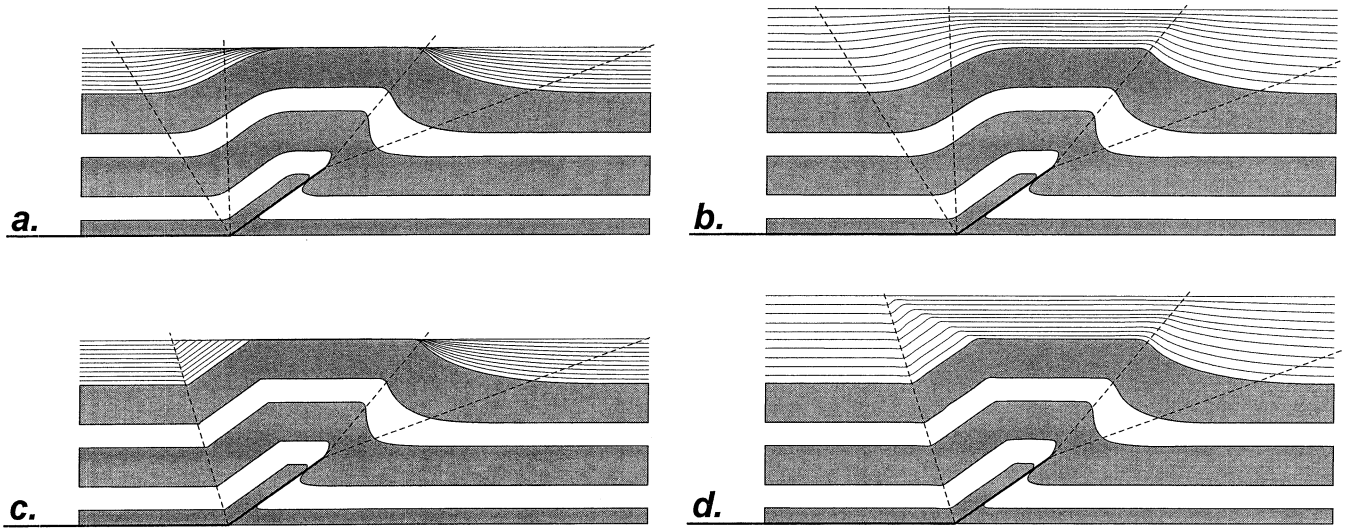

Fig. 4. Growth-strata geometries. Trishear fault-propagation fold: fault angle = 35°, forelimb trishear apical angle = 30°, $P/S = 1.5$ and symmetric backlimb trishear with 30° apical angle. (a) Sedimentation rate is equal to uplift rate. (b) Sedimentation rate is larger than uplift rate. (c) Equal to (a) but with backlimb trishear equal to zero (parallel-kink model). (d) Equal to (b) but with backlimb trishear equal to zero (parallel-kink model).

is very different (compare Fig. 4a with c and b with d). The growth triangles are not obvious in the backlimb trishear cases. The apparent truncation developed in the parallel-kink example of Fig. 4c is replaced by a smooth pinch-out toward the anticline crest (Fig. 4a). The growth triangle seen in Fig. 4d is replaced by a very diffuse zone (Fig. 4b).

4. Comparison with analog models

Several analog models (Morse, 1977; Chester et al., 1991; Ormand and Hudleston, 1999) have shown cases where an angular bend of the fault plane produces rounded fold geometries in the overlying layers (Figs. 1 and 5). Here we chose two examples to model, one from Chester et al. (1991) and the other from Morse (1977). By trial and error, reasonable approximations can be made.

Chester et al.'s (1991) model (Fig. 5a) can be fit well with a backlimb trishear zone that has apical angle of 40° and asymmetry of −20°. To illustrate the deformation associated with bedding thickness changes, we superimpose the final strain ellipses and the lines of no finite elongation (LNFEs) calculated with the backlimb trishear kinematics on a detailed view of the analog model (Fig. 5b). In the backlimb of the analog model, two major fracture sets form an angle of ~27°. The bisector of that angle is approximately parallel to the minor axis of the ellipses showing a good fit between the analog and the kinematic model. However, the LNFEs are parallel to minor fractures, but not to the major set. Chester et al.'s (1991) description of the evolution of this model shows that the fractures are generated near the fault bend and then rotated and translated onto the backlimb. If the principal fractures originated inside the backlimb trishear zone as shear and extension cracks, and then were rotated and translated up the ramp, the match between the analog and kinematic models are reasonably good.

We simulated Morse's (1977) analog model (Fig. 5c) with a backlimb trishear zone apical angle of 50° and asymmetry of −25°. The final strain ellipses and LNFEs calculated with the backlimb trishear kinematics also compare well with the analog model (Fig. 5d), particularly if we again consider that the fractures are generated inside the backlimb trishear zone and then translated.

In the analog examples we have analyzed, the backlimb trishear models that fit best always have a negative asymmetry that produces the thickening of the backlimb, generally accommodated by many back-thrusts. This is perhaps not surprising if one considers that the backlimb thickening probably represents a Coulomb shear zone conjugate to the thrust ramp. The kinematics of backlimb trishear is consistent with the back-thrust geometry observed only if these are generated inside the trishear zone and then translated. The model predicts that the back-thrusts generated in the backlimb (not in the trishear zone) must dip more steeply than those found in the examples analyzed.

5. Conclusions

We have presented a new kinematic model to produce rounded hanging wall backlimb folds above angular fault bends. The backlimb trishear model is area balanced and involves shear oblique to the bedding planes, implying that the beds progressively rotate over the fault bend. If backlimb trishear is symmetric with respect to the fault-bend bisector and the apical angle is zero the model reproduces

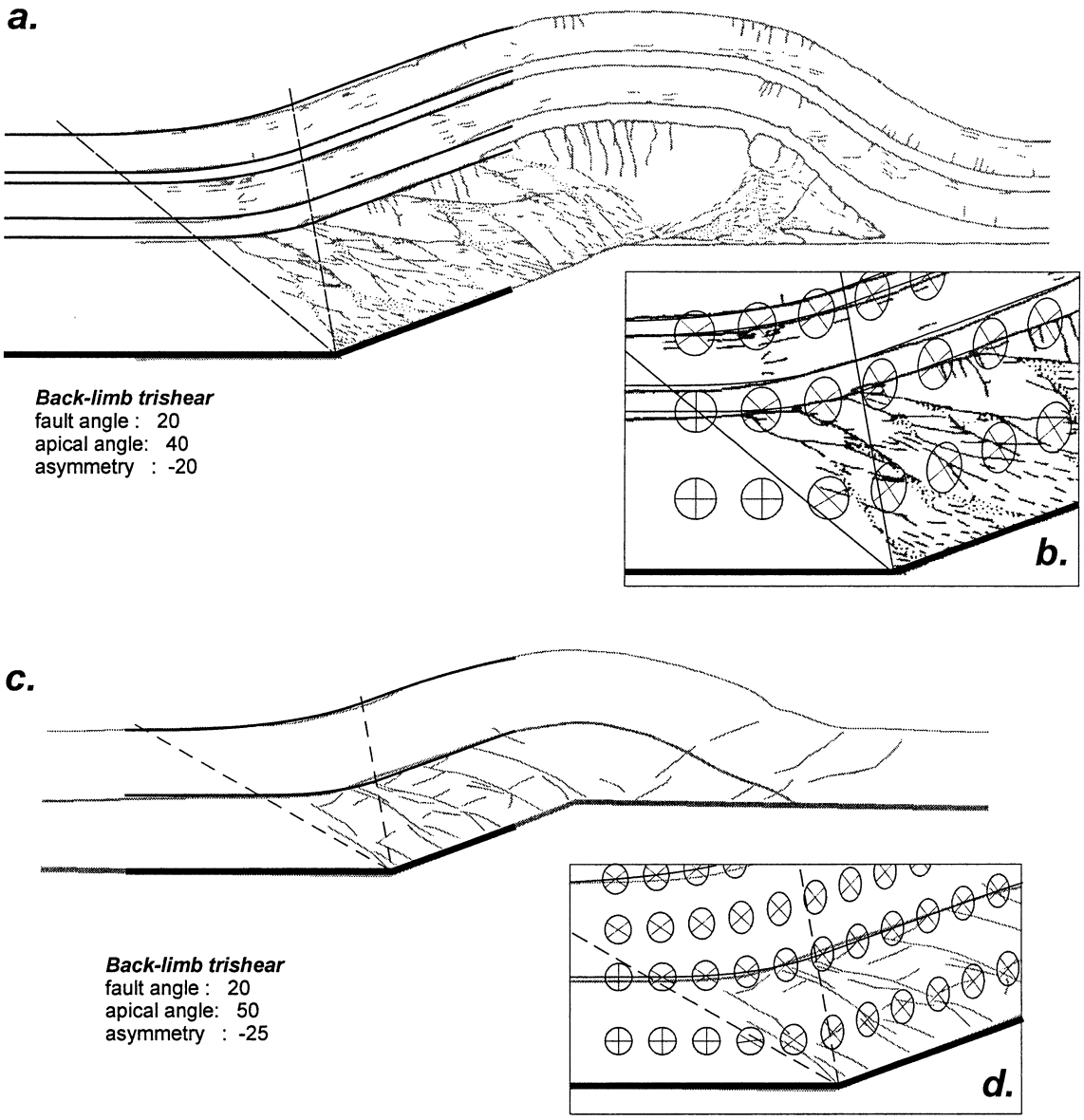

Fig. 5. Kinematic simulation of the analog experiments using the backlimb trishear model presented here. In all cases, the analog model is shown in gray and the backlimb trishear model overlaid in black. (a) Simulation of the Chester et al. (1991) experiment using a 40° apical angle and −20° of asymmetry. (b) Detail of (a) in which we show the final strain ellipses and the LNFEs (lines of no final elongation) calculated with the backlimb trishear kinematics. (c) Simulation of the experiment by Morse (1977) using a 50° apical angle and −25° of asymmetry. (d) Detail of (c) showing the final strain ellipses and the LNFEs superimposed on Morse's (1977) model.

the parallel-kink fault-bend fold (Suppe, 1983). If the zone is asymmetric and the apical angle is zero, the inclined shear model (White et al., 1986) is duplicated. Thus, the model is a more general way of describing backlimb kinematics than existing kinematic approaches.

Changes in bed thickening are greater in asymmetric backlimb trishear models, however they are also present in the symmetric cases. The growth-strata pattern generated with backlimb trishear indicates the progressive rotation of the beds and is clearly different than that produced by the parallel-kink model.

The model is consistent with analog experiments of fault-bend folds above angular fault bends. In both cases analyzed, the asymmetry of the backlimb trishear zone is always negative. Our model provides a sound and realistic kinematic treatment of bed thickening due to back-thrusts, a common feature observed in nature and experiments. The model also produces results consistent with mechanical analyses of fault-bend folds (Johnson and Berger, 1989).

Sharp bends in the fault planes are commonly not distinguishable on seismic reflection data. In the absence of such observations, an interpreter generally assumes that rounded hanging wall synclines require that the underlying fault be curved. However, field data, mechanical analysis and

experimental results, as well as the new kinematic analysis provided here, demonstrate that curved beds can be produced by angular fault bends.

Acknowledgements

We thank Judith Chester and Stuart Hardy for reviews of this manuscript. Supported by a grant to Cristallini from the Agencia Nacional de Promoción CientÍfica y Tecnológica (proyecto BID 802/OC-AR-PICT 00538) and NSF grant EAR-9814348 to Allmendinger. Acknowledgment is also made to the donors of The Petroleum Research Fund, administered by the ACS, for partial support of this research.

References

Berger, P., Johnson, A.M., 1983. First-order analysis of deformation of a thrust sheet moving over a ramp. Tectonophysics 70, T9–T24.

Chester, J.S., Logan, J.M., Spang, J.H., 1991. Influence of layering and boundary conditions on fault-bend and fault-propagation folding. Geological Society of America Bulletin 103, 1059–1072.

Erslev, E.A., 1991. Trishear fault-propagation folding. Geology 19, 617–620.

Hardy, S., 1995. A method for quantifying the kinematics of fault-bend folding. Journal of Structural Geology 17, 1785–1788.

Johnson, A.M., Berger, P., 1989. Kinematics of fault-bend folding. Engineering Geology 27, 181–200.

Mase, G.E., Mase, G.T., 1992. Continuum Mechanics for Engineers. CRC Press, Boca Raton.

Morse, J., 1977. Deformation in ramp regions of overthrust faults: experiments with small-scale rock models. In: Joint Wyoming–Montana–Utah Geological Associations Guidebook. Rocky Mountain Thrust Belt Geology and Resources. 29th Annual Field Conference, Wyoming Geological Association, pp. 457–470.

Ormand, C.J., Hudleston, P.J., 1999. Analog models of fault-bend folding: the effects of oblique ramping and tear faulting on hanging wall structures. Geological Society of America, Annual Meeting, 1999. Abstract 51868.

Serra, S., 1977. Styles of deformation in the ramp region of overthrust faults. In: Joint Wyoming–Montana–Utah Geological Associations Guidebook. Rocky Mountain Thrust Belt Geology and Resources. 29th Annual Field Conference, Wyoming Geological Association, pp. 487–498.

Suppe, J., 1983. Geometry and Kinematics of fault-bend folding. American Journal of Sciences 283, 684–721.

Suppe, J., Mendwedeff, D., 1990. Geometry and kinematics of fault-propagation folding. Eclogae geol. Helv 83, 409–454.

White, N.J., Jackson, J.A., McLemzoe, D.P., 1986. The relationship between the geometry of normal faults and that of the sedimentary layers in their hanging walls. Journal of Structural Geology 8, 897–909.

Zehnder, A.T., Allmendinger, R.W., 2000. Velocity field for the trishear model. Journal of Structural Geology 22, 1009–1014.